ResearchGate

See discussions, stats, and author profiles for this publication at: https://www.researchgate.net/publication/260520084

Theoretical Studies on the Interaction of Ruthenium Sensitizers and Redox Couple in Different Deprotonation Situations

ARTICLE *in* THE JOURNAL OF PHYSICAL CHEMISTRY A · MARCH 2014

Impact Factor: 2.69 · DOI: 10.1021/jp410220q · Source: PubMed

CITATIONS
4

READS
34

5 AUTHORS, INCLUDING:

Mo Xie
Jilin University
6 PUBLICATIONS **5** CITATIONS
SEE PROFILE

Fu-Quan Bai
Jilin University
124 PUBLICATIONS **435** CITATIONS
SEE PROFILE

Available from: Mo Xie
Retrieved on: 26 January 2016

THE JOURNAL OF PHYSICAL CHEMISTRY A

Article

pubs.acs.org/JPCA

Theoretical Studies on the Interaction of Ruthenium Sensitizers and Redox Couple in Different Deprotonation Situations

Mo Xie, Jie Chen, Fu-Quan Bai,* Wei Wei, and Hong-Xing Zhang*

State Key Laboratory of Theoretical and Computational Chemistry, Institute of Theoretical Chemistry, Jilin University, Changchun, 130023, People's Republic of China

Supporting Information

ABSTRACT: We report a DFT study of interaction between the Ru complex sensitizer [$Ru(dcbpy)_2(NCS)_2$: dcbpy = 4,4′-dicarboxy-2,2′-bipyridyl] (N3) and iodide ion under the influence of different deprotonation situations. There are two kinds of interaction mechanisms: iodide ion interacts with metal-center Ru atom or carboxyl, derived from the natural charge distribution analysis. The calculation indicated that there were several stable intermedium forms in different deprotonation degree. The stability of these intermedium forms would be perturbed gradually while the number of eliminated protons increased. It can be predicted that in the initial period of absorption and injection as well as the dissolve process where the deprotonation was demanded, the dye will not attacked by the iodide ion in solution extensively. Additionally, dye with more carboxyls will reduce the activity of redox reaction and more obstacles are required to be overcome before or during the redox reaction. The comparison of natural charge between isolate N3 and N3 with iodide ion intermedium ($N3I^-$) showed the iodide ion attacking made the charge contribute on N3 molecule more negative, nevertheless the $N3I^-$ still has ability to attract another iodide ion. The attacking of iodide ion will also influence the electronic transition and absorption properties through the analysis of the frontier molecular orbitals and the densities of states. The results reported in this paper give us the guidance to carry out the further investigations about the dye regeneration process.

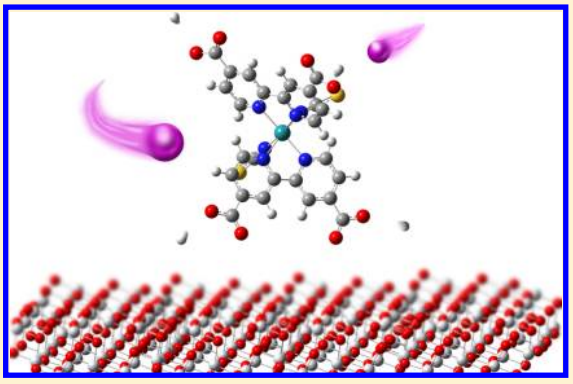

1. INTRODUCTION

Dye-sensitized solar cells (DSSCs) have been the subjects of intensive study ever since the discovery by Grätzel and co-workers[1] in the 1990s, which attracted much attention due to their low cost and high efficiency.[2,3] DSSCs are typically compose of five components: dye sensitizer, mesoporous semiconductor metal oxide film, electrolyte transporter, photoanode, and counterelectrode. The cell operation is achieved by following major steps: under the condition of visible light, the dye sensitizer which is in the ground state is stimulated to an excited state by absorbing photon. After that, the photoexcited electron injects into the conduction band of semiconductor that dye sensitizer anchors to. Then the injected electron diffuses from semiconductor passing through the electrode and the external load, finally to the counter electrode, completing the circuit. Meanwhile, the oxidized dye molecule is regenerated by the electrolyte which accepts the electron from the counter electrode.[4] Unhindered and favorable dye regeneration will be helpful to expand the lifetime of DSSC.

The I^-/I_3^--based ruthenium dyes are one of the most widely used sensitizers, whose energy conversion efficiency reaches over 11%[5−8] up to now. As representatives of ruthenium dyes, N3 [$Ru(dcbpy)_2(NCS)_2$: dcbpy = 4,4′-dicarboxy-2,2′-bipyridy]and its derivatives are the research hotspot and were improved deeply because of their wide absorption in the visible and near-infrared regions. Not merely by virtue of experiment method, N3 and its derivatives are also investigated in point of the orbitals energy level, molecule modification and spectral properties by theoretical calculation extensively.[9−15] Moreover, the redox couple as a typical electrolyte is indispensable in improving the performance of the cells as well. The redox couple is a medium to transfer electrons from the counter electrode to the oxidized dye so that to affect the open-circuit voltage (V_{oc}) by controlling the potential difference of the I^-/I_3^- redox couple correspond to both counter electrode and semiconductor, significantly. In addition, the interaction between the I^-/I_3^- redox couple and dyes is primarily employed as the regulation of dye regeneration. As a consequence, the reaction mechanism and weak interaction between the I^-/I_3^- redox couple and other cell components draw lots of attention of researchers in recent years.

In previous work by Clifford et al.[16] dye regeneration reaction was proposed constituted by two steps and yield an intermediate complex [dye^+,I^-] throughout the process.

$$dye^+ + I^- \rightarrow [dye^+, I^-] \quad (1)$$

Received: October 15, 2013
Revised: February 22, 2014
Published: March 4, 2014

 © 2014 American Chemical Society dx.doi.org/10.1021/jp410220q | J. Phys. Chem. A 2014, 118, 2244−2252

$$[dye^+, I^-] + I^- \rightarrow dye + I_2^- \quad (2)$$

According to the reported prediction, the short-lived intermediate $[dye^+,I^-]$ could be a seven-coordinate complex with a covalent Ru−I bond or based upon pairing or specific π-interaction. Then, two possible intermediate pathway: inner-sphere and outer-sphere were demonstrated by Privalov and co-workers.[17] Two different interaction modes:I^- coordinated to Ru(III) center and I^- ligand exchanged the thiocyanogen group (NCS), were included in the inner-sphere pathway. The other two:I^-interacted with the *dcbpy* ligand directly and I^- reacted with NCS ligand via bonding S atom, were included in the outer-sphere pathway. Hu et al.[18] also focused on the intermediate pathway and promote their results by extending electrolyte field from I^-/I_3^- to X^-/X_3^- (X = Br, I, At). There was no certain conclusion about reaction site of regeneration, yet one or two appropriate situations were chosen by some reporters to clarify their research.[19,20] Thus, more attempts are needed in order to seek the comprehensive possibility of regeneration reaction and these attempts should be taken in different perspective by different methods. Moreover, dye regeneration is a complicated process including the participation of more than one cell components and is influenced by the circumstances where it occurs. In the recent study of Kusama et al.[21] one tetrabutylammonium(TBA) group was bonded to one of three NCS ligands in optimization of a series of complexes to better stimulate the real condition of solution. Besides the counterion, the effects of deprotonation are indispensable in observing the behaviors of dyes and redox couples. The deprotonation generate when dye molecules dissolved and absorbed.[22] It is the initial period of cell cooperation and in this period, the situation of dye regeneration reactants will be confirmed. However, few studies have been investigated the deprotonation effect to the redox reaction. Here the dehydrogenation mainly occurs on the neutral dye, so the neutral dye is also the subject of great research value. The neutral dyes, initially, coexit with the oxidized and excited dyes in electrolyte solution throughout entire cell reaction process, the interaction between neutral dyes and I^-/I_3^- redox couples would affect the concentration of iodide and dye molecules, thus affect the dye regeneration process. Then, the forms of neutral dyes and I^-/I_3^- redox couples before the redox reactions proceeds such as the reaction distance would influence the interactions between oxidized or excited dyes and redox couples immediately. It is helpful for us to contribute a beneficial reaction environment for dye regeneration.

In this study, theoretical calculations were employed to explore the deprotonation effect upon the interactional behavior between N3 dye and iodide ion. In addition, we discussed the potential locations of iodide ion around the N3 dye molecule in different degrees of dehydrogenation depending on the distribution of natural charges of N3 dye. The four carboxyl groups were marked as *a*, *b*, *c*, and *d* to describe the different situations of deprotonation clearly. We aimed at seeking out the combination trend of neutral dye with iodide ion in different attaching points under the influence of different degrees of dehydrogenation. DFT-based theoretical studies of electronic structures and thermodynamic properties were used to obtain the results in this paper.

2. COMPUTATIONAL DETAILS

Density function theory (DFT) was applied here for the geometry optimization and electronic structure calculations of the objected complex. The geometry structures of the complexes were optimized by employing M06-2X[23] function in vacuo. The "double-ξ" basis set LanL2DZ consisting of 18 valence employed associated with the pseudopotential was employed for Ru atom. SDDAll basis set was employed for I atom and the 6-31g(d) basis sets was employed for other atoms.

Scheme 1. Chemical Structure of N3 Dye

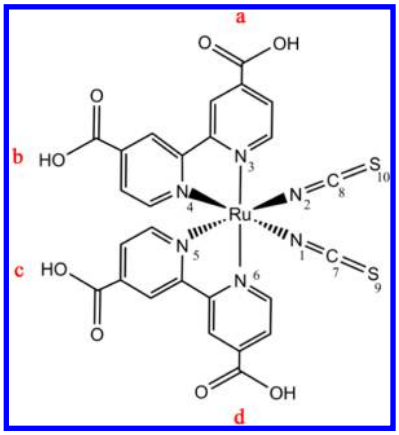

The M06-2X function has been compared with CAM-B3LYP[24] and X3LYP[25] in geometry optimization and charge analysis. There were more or less structural distortions by using all the three functions and M06-2X function performed mediocre. Meanwhile, the relatively low energy was achieved by using the M06-2X function. Furthermore, M06-2X functional has been proved to have preferable performance in describing the intermolecular interactions.[26−28] Thus, the M06-2X functional was finally adopted to obtain all the results.

An NBO analysis[29] was performed to provide insight into the atom charge and electron density by employing M06-2X functional as well and basis sets were mentioned before. All calculations were achieved with the Gaussian 09 program package.[30]

3. RESULTS AND DISCUSSION

3.1. Geometric Structures and NBO Analysis of Neutral N3 Dye. The geometry optimization of neutral N3 dye was adopted *C2* symmetry in vacuo. As shown in Figure 1 the optimized complex take a pseudo-octahedral coordination and the Ru atom occupies the center. Comparing with the previous study,[17] the optimized N3 dye has a relatively high symmetry so that the Ru−N bond distances of the symmetric positions were same, the bond lengths of them were 2.058 Å for Ru−N1 and Ru−N2, 2.082 Å for Ru−N3 and Ru−N6, and 2.085 Å for Ru−N4 and Ru−N5, respectively.

The natural population analysis (NPA) was employed to explore the properties of $N3I^-$ intermedium (isolate N3 dye combined with iodide ion) from the point of electrostatic interaction. Some representative atoms and groups with their natural charge are listed in Table 1. The natural charge located at metal center Ru atom is 0.211e so that Ru becomes a positive center in a small region which composed by Ru atom and negative N atoms around. The most positive natural charges are located at C atoms of carboxyl, 0.860e for carboxyl *a* and *d* and 0.858e for carboxyl *b* and *c*. The H atoms of carboxyl have the similar natural charge, 0.521−0.522e. The natural charge data of groups are the sum of data of all atoms which the group are consisted by.

dx.doi.org/10.1021/jp410220q | J. Phys. Chem. A 2014, 118, 2244−2252

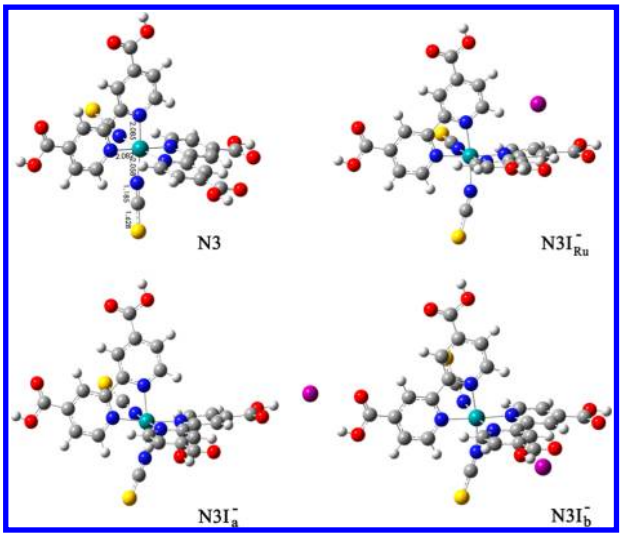

Figure 1. Optimized geometries of N3 dye and N3I$^-$ intermediums (neutral N3 dye combined with iodide ion) in different forms.

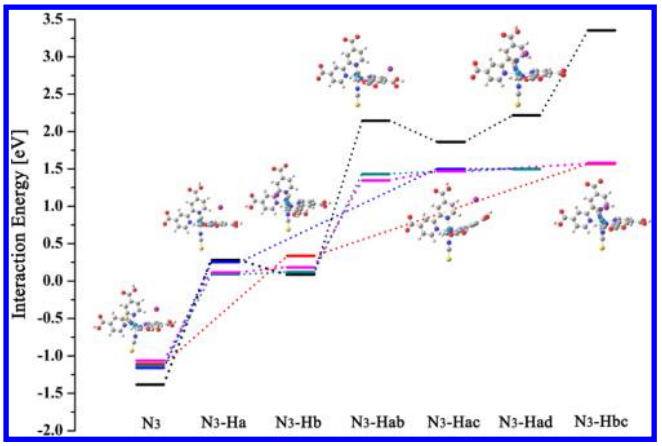

Figure 2. Calculated interaction energies (eV) and representative structures of N3I$_{Ru}^-$ (neutral and deprotonated N3 dye combined with iodide ion) system. Color of energy level: N3I$_{Ru}^-$, black; N3I$_a^-$, red; N3I$_b^-$, blue; N3I$_c^-$, green; N3I$_d^-$, magenta.

As shown in Table 1, the similar geometric groups with the identical natural charge are obtained. This is due to the relatively high symmetry which is not merely expressed in the geometrical configurations. Furthermore, Figure 2 shows the total electronic density. The electrons mainly localized on N atoms, O atoms and NCS ligands, on the contrary, positive charge centralized on Ru metal center and C, H atoms of carboxyl. Taking electrostatic interaction and steric hindrance into consideration, Two ways that iodide ion approached the neutral N3 molecule was first designed. One was iodide ion attacked the Ru atom from the middle area between two *dcbpy* ligands (Ru position), the other was the iodide ion horizontally approached the carboxyl through H atom (carboxyl position). It can be noted, there were two different carboxyl positions as a result of different chemical circumstances even though the natural charge localized on H atoms of carboxyls are the same. However the carboxyls were identified as anchor groups[22] which connected dye sensitizers and semiconductor films as a channel that electron injected from dye to semiconductor. As a result, the NCS ligand was also a probably beneficial position where iodide ion approached the N3 molecule. The similar trial

Table 1. Natural Charges (e) for Main Atoms and Groups

atoms and groups	N_3	N_3 ($-H_a$)	N_3 ($-H_b$)	N_3 ($-H_{ab}$)	N_3 ($-H_{ac}$)	N_3 ($-H_{ad}$)	N_3 ($-H_{bc}$)
Ru	0.211	0.264	0.246	0.259	0.254	0.257	0.247
C(a)	0.860	0.818	0.861	0.817	0.819	0.818	0.863
(b)	0.858	0.861	0.818	0.817	0.863	0.863	0.819
(c)	0.858	0.864	0.863	0.865	0.818	0.863	0.819
(d)	0.860	0.865	0.863	0.865	0.863	0.818	0.863
H(a)	0.521		0.513				0.507
(b)	0.522	0.513			0.507	0.508	
(c)	0.522	0.514	0.516	0.510		0.508	
(d)	0.521	0.513	0.515	0.509	0.507		0.507
N1	−0.513	−0.500	−0.501	−0.491	−0.485	−0.478	−0.486
N2	−0.513	−0.479	−0.490	−0.464	−0.475	−0.478	−0.488
N3	−0.351	−0.395	−0.367	−0.401	−0.388	−0.393	−0.358
N4	−0.346	−0.357	−0.389	−0.391	−0.352	−0.354	−0.381
N5	−0.346	−0.354	−0.344	−0.336	−0.384	−0.354	−0.382
N6	−0.351	−0.368	−0.351	−0.350	−0.364	−0.393	−0.357
C7	0.175	0.166	0.176	0.183	0.190	0.184	0.183
C8	0.175	0.158	0.174	0.170	0.170	0.183	0.184
S9	−0.263	−0.310	−0.322	−0.359	−0.353	−0.355	−0.356
S10	−0.263	−0.322	−0.312	−0.354	−0.360	−0.355	−0.355
COOH(a)	0.055		0.041				0.025
(b)	0.054	0.041			0.026	0.026	
(c)	0.054	0.043	0.043	0.027		0.026	
(d)	0.055	0.042	0.042	0.026	0.024		0.025
SCN(1,7,9)	−0.601	−0.645	−0.647	−0.667	−0.648	−0.650	−0.660
(2,8,10)	−0.601	−0.643	−0.628	−0.648	−0.665	−0.650	−0.660
dcpby(a,b)	0.496	−0.430	−0.426	−1.350	−0.468	−0.479	−0.462
(c,d)	0.496	0.454	0.456	0.407	−0.473	−0.478	−0.465

dx.doi.org/10.1021/jp410220q | J. Phys. Chem. A 2014, 118, 2244−2252

Table 2. Optimized Geometry Parameters of $N3I_{Ru}^-$ (Isolate N3 Dye Combined with Ru Position Iodide Ion) System Species (Bond in Å; Angle in deg)

parameter	N3	N3−I^-	N3− I^- (−H_a)	N3− I^- (−H_b)	N3−I^- (−H_{ab})	N3−I^- (−H_{ac})	N3−I^- (−H_{ad})	N3−I^- (−H_{bc})
Ru−I		5.555	5.632	5.554	6.868	6.965	6.296	4.892
I−N1		7.043	7.082	6.866	7.711	8.667	7.903	6.568
I−N2		6.845	6.844	7.223	8.266	7.200	7.918	6.594
I−N3		7.008	7.055	4.767	8.494	8.376	6.372	5.283
I−N4		4.747	4.817	4.703	6.775	5.750	4.946	3.872
I−N5		4.631	4.767	4.509	5.661	7.190	4.977	3.818
I−N6		4.514	4.526	6.759	5.362	5.661	6.686	5.181
Ru−N1	2.058	2.106	2.117	2.133	2.142	2.120	2.125	2.140
Ru−N2	2.058	2.099	2.112	2.117	2.124	2.128	2.126	2.144
Ru−N3	2.082	2.116	2.118	2.101	2.113	2.118	2.129	2.104
Ru−N4	2.085	2.106	2.106	2.113	2.114	2.119	2.111	2.126
Ru−N5	2.085	2.116	2.105	2.100	2.098	2.122	2.109	2.127
Ru−N6	2.082	2.100	2.113	2.108	2.123	2.119	2.128	2.098
N1−C7	1.185	1.174	1.173	1.173	1.172	1.172	1.171	1.171
C7−S9	1.628	1.640	1.646	1.647	1.651	1.651	1.652	1.653
N2−C8	1.185	1.175	1.173	1.173	1.172	1.172	1.172	1.171
C8−S10	1.628	1.639	1.646	1.646	1.652	1.650	1.652	1.651
N1−Ru−N2	92.7	93.6	93.4	92.2	91.8	91.4	92.7	90.2
S9−Ru−S10	105.5	100.7	100.0	94.2	93.0	91.5	98.9	87.7
I−Ru−N3−N4		32.6	34.0	55.4	59.3		42.8	48.9
I−Ru−N6−N5		52.9	54.4	37.4	32.2	99.0	41.5	48.0
N4−Ru−N6−N5	91.9	87.0	86.5	93.7	88.5	91.7	83.5	96.4

has been done by Kusama et al.[20,21] Then, iodide ion attacked the NCS ligands horizontally and vertically became the third way we explored in consider of the comprehensive attack sites.

Figure 1 shows the optimized geometries of $N3I^-$ intermediums (A, Ru position; B, carboxyl *a* position; C, carboxyl *b* position), their structures and energies will be discussed in detail combined with the deprotonation influence later. The third way that the iodide ion interacts with the N3 molecule through NCS ligand either turns into the first two ways or is not stable, so it will not be thoroughly discussed in this paper.

3.2. Attack on Ru Position: Geometry and Energy Analysis. The full optimized geometry of $N3I_{Ru}^-$ intermedium (isolate N3 dye combined with Ru position iodide ion) is given in Figure 1 and its main bond distances and angles are listed in Table 2. Iodide ion was situated in the middle of two *dcbpy* ligands and closed to the one that contained two N atoms marked N3 and N4. As can be seen from the bond distances of series Ru−N bonds, symmetry of N3 molecule was broken by iodide ion obviously and the Ru−N bonds for $N3I_{Ru}^-$ intermedium were stronger than for isolated N3 dye. The N−C, C−S bonds were vibrating competitively over time and the geometry of intermedium relatively stabilized when N−C, C−S distances were about 1.174 and 1.640 Å respectively. The angles of N1−Ru−N2 and S9−Ru−S10 showed that the two NCS ligands were not vertical in optimized isolated N3 geometry and the angle between them was over 90°. But this situation was improved after iodide ion appeared in the system.

There were two different deprotonation patterns when one proton was eliminated in view of the symmetry and chemical circumstance; they were N3 without H_a or H_b. Similarly, when two protons were eliminated, four patterns were taken into account, N3 without H_aH_b, H_aH_c, H_aH_d or H_bH_c. The natural charges of their main atoms and groups were also listed in Table 1. The natural charges located on Ru atom did not turn to negative but increased a little bit affected by deprotonation. It is still capable for Ru metal center to attract iodide ion. Nevertheless, at least one of *dcpby* ligands turned to negative after deprotonation and this factor might be disadvantageous for the stability of whole system. For $N3I_{Ru}^-$−H_a ($N3I_{Ru}^-$ intermedium without H_a), the position of iodide ion did not deviate from that in $N3I_{Ru}^-$ system obviously. The iodide ion in $N3I_{Ru}^-$ − H_b was localized on the opposite side of the iodide ion that in $N3I_{Ru}^-$−H_a from the N1−Ru−N4 axis and closed to the other *dcbpy* ligand. The bond distances of Ru−N4 and Ru−N5 are shorter than other Ru−N bonds in $N3I_{Ru}^-$−H_a. But it is regular to the bond distances of the Ru−N bond series in $N3I_{Ru}^-$−H_b. The bond lengths both for $N3I_{Ru}^-$−H_a and $N3I_{Ru}^-$−H_b are about 0.007 Å longer than that for $N3I_{Ru}^-$ while the N−C bonds of NCS ligands are maintained.

The position of the iodide ion for $N3I_{Ru}^-$−H_{ab} ($N3I_{Ru}^-$ intermedium without H_a and H_b) is similar to that of $N3I_{Ru}^-$−H_a besides that the iodide ion was more far away from the metal Ru center. For $N3I_{Ru}^-$−H_{ad} and $N3I_{Ru}^-$−H_{bc}, the iodide ion was almost located on the flat surface that contained Ru, N1, and N2 atoms. In $N3I_{Ru}^-$−H_{ac}, in particular, the iodide ion was coplanar with the *dcbpy* ligand (containing the carboxyl *a* and *d*) and sited right above carboxyl (*d*) ligand. It is worth noting that the angle between the two *dcbpy* ligands of $N3I_{Ru}^-$−H_{ad} was 83.5°, smaller than 90° and in $N3I_{Ru}^-$−H_{bc}, on the contrary, was 96.4° (Figure S1 of the Supporting Information).

The interaction energies between iodide ion and N3 molecule or N3 without protons and their corresponding geometries were illustrated in Figure 2. It is −1.385 eV when the iodide ion interacted with neutral N3 molecule, so we conjectured that $N3I_{Ru}^-$ intermedium is more stable than the sum of isolated N3 molecule and isolated iodide ion. The interaction energy is positive under the dehydrogenation situations and numerical values when two protons were eliminated are at least one order of magnitude larger than

dx.doi.org/10.1021/jp410220q | J. Phys. Chem. A 2014, 118, 2244−2252

Table 3. Optimized Geometry Parameters of $N3I_{car}^-$ (Isolate N3 Dye Combined with Carboxyl Position Iodide Ion) System Species (Bond in Å; Angle in deg)

			(a)					
attacking position of I	parameter	N3	N3−H_a	N3−H_b	N3−H_{ab}	N3−H_{ac}	N3−H_{ad}	N3−H_{bc}
I_a	I−H	2.368		2.498				2.608
	I−O_y[b]	4.212		4.454				4.461
	Ru−N1	2.145		2.133				2.127
	Ru−N3	2.101		2.101				2.118
	Ru−N4	2.105		2.11				2.116
	N1−C7	1.179		1.175				1.172
	C7−S9	1.635		1.641				1.648
	N1−Ru−N2	97.6		93.8				91.4
	S9−Ru−S10	119.3		101.3				91.5
	I−H−O_x[a]	168.9		162.0				163.9
	I−O_x[a]−C−O_y[b]	−6.9		4. 2				2.7
	N4−Ru−N6−N5	95.7		86.3				89.0
I_b	I−H	2.376				2.633	2.575	
	I−O_y[b]	4.323				4.606	4.489	
	Ru−N1	2.142				2.120	2.120	
	Ru−N3	2.097				2.115	2.126	
	Ru−N4	2.112				2.116	2.117	
	N1−C7	1.179				1.172	1.172	
	C7−S9	1.634				1.649	1.649	
	N1−Ru−N2	95.6				91.9	93.2	
	S9−Ru−S10	116.8				92.9	98.9	
	I−H−O_x[a]	165.5				158.7	161.6	
	I−O_x[a]−C−O_y[b]	3.833				−2.2	−2.8	
	N4−Ru−N6−N5	92.0				90.1	89.5	
			(b)					
attacking position of I	parameter	N3	N3−H_a	N3−H_b	N3−H_{ab}	N3−H_{ac}	N3−H_{ad}	N3−H_{bc}
I_c	I−H	2.378	2.445	2.470	2.466		2.548	
	I−O_y[b]	4.244	4.279	4.370	4.212		4.442	
	Ru−N1	2.085	2.103	2.115	2.137		2.112	
	Ru−N3	2.108	2.110	2.105	2.107		2.131	
	Ru−N4	2.123	2.107	2.117	2.111		2.101	
	N1−C7	1.176	1.174	1.174	1.173		1.172	
	C7−S9	1.634	1.642	1.642	1.649		1.6	
	N1−Ru−N2	95.5	93.8	92.0	92.1		93.4	
	S9−Ru−S10	117.7	98.9	94.3	93.2		98.6	
	I−H−O_x[a]	168.9	167.3	165.2	169.8		162.6	
	I−O_x[a]−C−O_y[b]	−2.1	6.4	−1.3	−1.1		−1.3	
	N4−Ru−N6-N5	94.6	89.1	89.5	88.7		90.2	
I_d	I−H	2.373	2.487	2.466	2.486	2.608		2.568
	I−O_y[b]	4.115	4.333	4.297	4.219	4.478		4.341
	Ru−N1	2.104	2.097	2.125	2.133	2.112		2.127
	Ru−N3	2.126	2.120	2.109	2.111	2.126		2.099
	Ru−N4	2.115	2.114	2.121	2.112	2.098		2.125
	N1−C7	1.176	1.174	1.174	1.173	1.172		1.172
	C7−S9	1.636	1.640	1.643	1.649	1.649		1.650
	N1−Ru−N2	96.8	96.1	93.7	92.8	93.1		91.5
	S9−Ru−S10	113.5	113.7	101.4	98.5	98.8		91.7
	I−H−O_x[a]	172.2	166.8	167.7	168.5	163.1		167.0
	I−O_x[a]−C−O_y[b]	6.5	5.0	1.4	8.3	3.5		1.0
	N4−Ru−N6−N5	95.8	92.9	88.6	87.4	87.2		9.2

[a]Single bond oxygen in carboxyl. [b]Double bond oxygen in carboxyl.

those without one proton. It was suggested that the stability was decreased while the deprotonation degree increased.

3.3. Attack on Carboxyl Position: Geometry and Energy Analysis. In this section, the carboxyl positions that iodide ion attacked increased to four which influenced by different situation of deprotonation. I_a, I_b, I_c, and I_d will indicate the four attack positions of iodide ion. Six deprotonation patterns (from zero to two) will still be indicated as H_a, H_b, H_{ab}, H_{ac}, H_{ad}, and H_{bc}. From the analysis of natural population, the carboxyl where dehydrogenation occurred was not appropriate for iodide attacking. The natural charges of other carboxyl groups were diminished at different levels influenced by

dx.doi.org/10.1021/jp410220q | J. Phys. Chem. A 2014, 118, 2244−2252

deprotonation and this would lead to more difficult attack for iodide ion. Table 3 showed the main bond distances and angles of all possibilities that four iodide ion positions combined with six deprotonation patterns. The intermolecular I−H distances for $N3I_a^-$ (isolate N3 dye combined with carboxyl *a* position iodide ion),$N3I_b^-$, $N3I_c^-$ and $N3I_d^-$ are about 2.37−2.38 Å and the values turned to 2.45−2.63 Å after H atoms were removed. But all values of distances above are longer than the van der Waals radii of bonding atoms, 3.78 Å.[31] It is worth noting that I, H, and O_x atoms do not possess a linear pattern and the angles of I−H−O_x ranged from 160° to 172° for all configurations. Then, we chose dihedral angle I−O_x−C−O_y to verify whether the iodide ion is coplanar with the carboxyl that it interacts with. The result indicate the coplanarity is better in $N3I_b^-$ and $N3I_c^-$ system than that in the $N3I_a^-$ and $N3I_d^-$ system.

The bond distances of Ru−N for all the structures are irregular and these values ranged from 2.10 to 2.16 Å. Similar to $N3I_{Ru}^-$ system, the N−C bond and C−S bond are getting longer and smaller with the increasement of dehydrogenation number, respectively. The angles of N1−Ru−N2, S9−Ru−S10, and the dihedral angle N4−Ru−N6−N5 are far from 90° for all four configurations when dehydrogenation number is zero and this phenomenon is getting better with the increasement of dehydrogenation number. To varying degrees, there are structural distortions for N3 molecule in interaction system compared with neutral N3 molecule in all geometries (Figure S1 of the Supporting Information).

The interaction energies of four systems are all shown in Figure 2. Taking the I_d series for example, the energy of $N3I_d^-$ is −1.064 eV which indicating the intermedium is relative stabilized and the value turns to positive when one proton was eliminated and it grows enormous when the eliminated protons increased to two. This result, considering order of magnitude, is coincide with $N3I_{Ru}^-$ system that have been discussed before. We can see the influences in interaction energies by different dehydrogenation numbers, obviously. The situations of other three systems are almost the same and we should also notice that the energies of four carboxyl position in condition of two deprotonation level are 1.5 eV or so unlike the more complicated Ru position.

From the above analysis, the attraction between N3 dye and iodide is weakened along with the eliminated protons increased. The dissociative iodide will deviate from the dye so that much more time is needed for iodide ion to approach the oxidized dye after charge injection. The numbers of carboxyl probably affect the redox reaction time and then affect the cell reaction efficiency. When the deprotonation degree continue to increase, the combination between N3 dye and iodide ion become extremely difficult. The interaction energies of these high deprotonation level forms would be larger than those at present judging from the interaction energy increase trend from Figure 2. It is suggested that the kinds of $N3I^-$ under high deprotonation degrees scarcely exist.

3.4. Charge Distribution of Intermediums. The total electronic density gives some hints about the charge distribution of the $N3I^-$ intermediums. As can be seen from Figure 3, for neutral N3 molecule, the charges located on *dcpby* ligands are positive or negative alternately and the distribution trends to uniform after iodide ion attack. This phenomenon is more obvious in the $N3I_{Ru}^-$ intermedium than $N3I_{car}^-$ (car refers to carboxyl) intermediums. Similarly, the Ru metal center, NCS ligands and carboxyl ligands become more negative affected by the iodide ion. As the iodide ion approaches closer to the center of dye molecule, $N3I_{Ru}^-$ intermedium seems more negative than both two $N3I_{car}^-$ intermediums. Even so, there are charges located on the H atoms in carboxyl ligands, it is not quite difficult to attract another iodide ion for $N3I^-$ intermediums. Therefore, the possible existences of other iodide ions around the intermedium can sustaine the redox reaction actively.

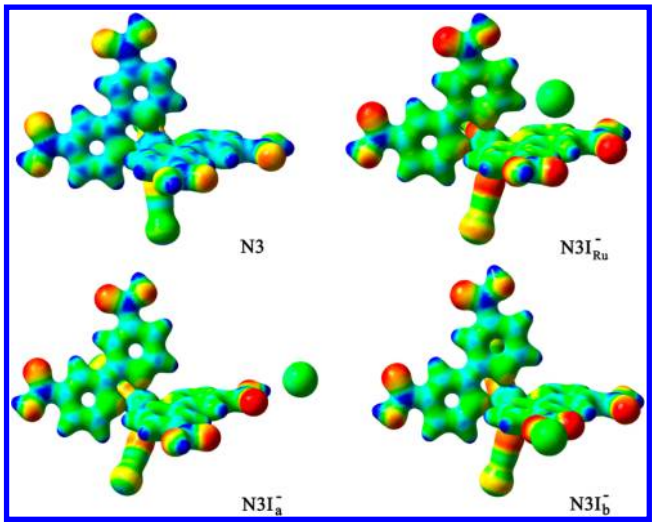

Figure 3. Map of total electronic density of N3 molecule and $N3I^-$ intermediums (blue, positive; red, negative).

For the iodide ion, the charge located is almost −1. The ionic radius of it is relatively large, so it is possible to reject another negative iodide ion. Thus, it can be predicted the second iodide ion which is involved in the second redox reaction step will not approach the intermediums before the electronic excitation and injection.

It will be useful to examine the frontier molecular orbitals (FMOs) of the intermediums to estimate the possible effects of iodide ion on the electronic excitation. The energy level and character of the selected FMOs are given in Figure 4 and Figure 5. The highest occupied molecular orbital (HOMO) and the lowest unoccupied molecular orbital (LUMO) of N3 molecule are contributed by the *dcpby* ligands and NCS ligands, respectively. When the iodide ion attack on Ru position, the

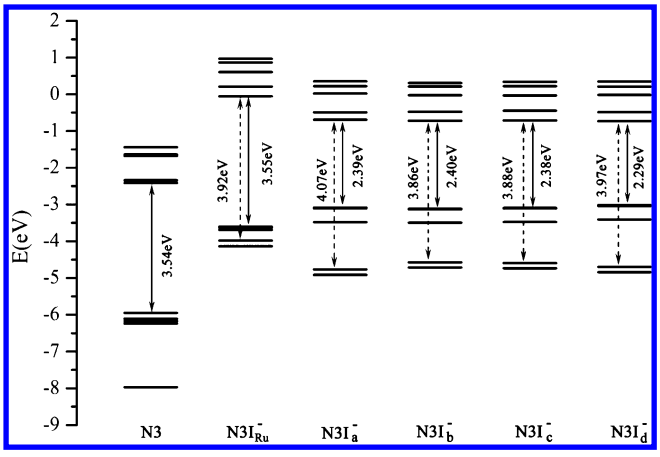

Figure 4. Molecular orbital energy level diagrams. Solid and dotted arrows denote the energy gaps between HOMO and LUMO, HOMO-3, and LUMO (they all localized on N3 molecule and correspond to the HOMO−LUMO gap in isolated N3), respectively.

dx.doi.org/10.1021/jp410220q | J. Phys. Chem. A 2014, 118, 2244−2252

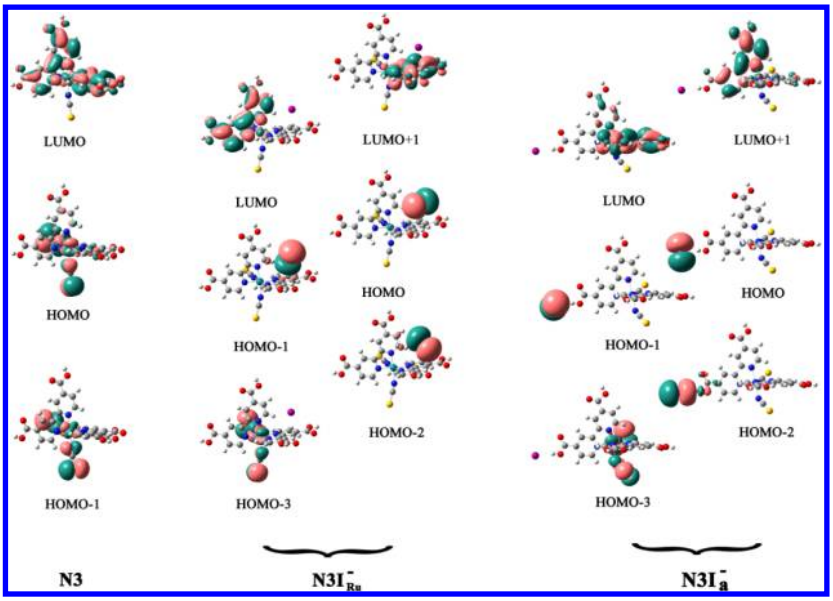

Figure 5. Selected frontier occupied and virtual molecular orbitals of N3 molecule and $N3I^-$ intermediums.

HOMO, HOMO-1, and HOMO-2 all localize on the iodide ion and LUMO, LOMO+1 can be regard as two parts of the original LUMO of N3 molecule. As a result, the HOMO and LUMO energy levels both increase and the band gap remains basically. It is possible to initiate the electronic transition from iodide ion to N3 molecule if the intermedium absorbs the energy same as the N3 transition energy. In other words, higher energy (3.92 eV) is needed to accomplish the electronic transition from *dcpby* ligands to NCS ligands (intramolecular transition) in intermediums. There are some differences in carboxyl position system, taking $N3I_a^-$ for example, the HOMO-2 is the mixed orbital composed of iodide ion and carboxyl, and the energy of which is much lower than HOMO and HOMO-1. Compared with $N3I_{Ru}^-$, the band gap of $N3I_a^-$ is much smaller, whereas the energy level difference between HOMO-3 and LUMO is larger than $N3I_{Ru}^-$ and N3. Hence, the intermolecular transition is more favorable than intramolecular transition. From the above analysis, the frontier molecular orbitals are influenced by iodide ion. Thus, it can be deducted that the iodide ion will cause a red shift of N3 absorption spectra and it would probably contribute the absorption transition in low energy region.

To research the iodide ion effect on molecular orbital deeply, the total and partial densities of states (DOS) of intermediums have been calculated and showed in Figure 6. The comparison between N3 and intermedium shows that the energy of both N3 occupied and virtual states increase after iodide ion attacked and this phenomenon is more obvious in $N3I_{Ru}^-$. Moreover, it is easy to discover that the last occupied states are contributed by iodide ion for two intermedium forms. This analysis of DOS can also obtain the results we discussed above. However, there is partial occupied state overlap from iodide ion and N3 components in $N3I_{Ru}^-$ while there is almost no overlap in $N3I_a^-$ intermedium. These properties would influence the charge injection and the influence involving the participation of TiO_2 will be discussed in detail later.

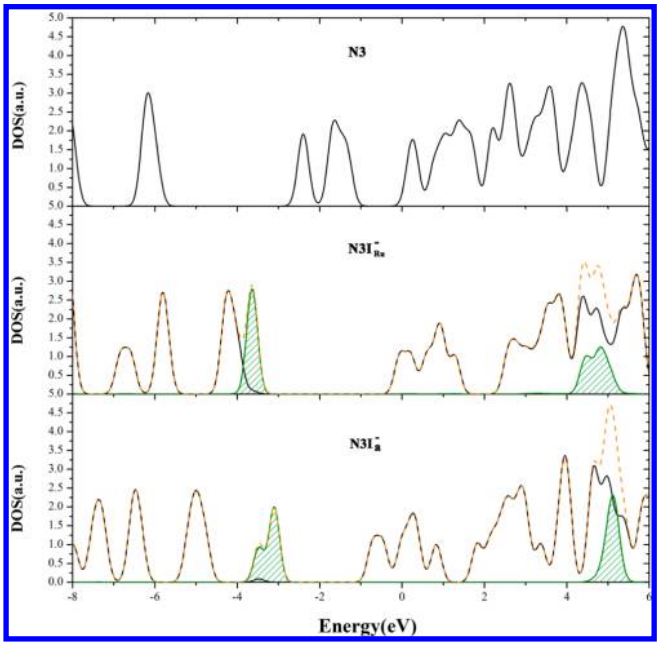

Figure 6. Total and partial densities of states of N3 molecule and $N3I^-$ intermediums. Orange dash, black solid, and olive shadow represent the contribution from total intermedium, partial N3, and iodide ion, respectively.

4. CONCLUSION

In order to understood the interaction between redox couple and isolate dye, we investigated the structures and energies of two $N3I^-$ intermidium forms under the influence of different degrees of deprotonation, Two kinds of relative stabilized structures, Ru position and carboxyl position, were found through the analysis of NBO charge. For the Ru position system, when dehydrogenation degree increased, the process of the iodide ion approaching the N3 molecule without protons became more difficult. At the same time, the interaction energy turned from negative to positive and the numerical value gradually increased. For the carboxyl position system, the deprotonation effect rarely influenced the geometrical configurations but the influence in interaction energies was still notable. Thereby, we conjecture that varieties of $N3I^-$ scarcely exist when more protons were eliminated sequentially.

dx.doi.org/10.1021/jp410220q | J. Phys. Chem. A 2014, 118, 2244−2252

Considering the surroundings including dyes and I^-/I_3^- redox couple and the cell mechanism, we infer that iodide ion will not attack the dye in initial stage of absorption and injection as well as the dissolving process. Furthermore, the numbers of carboxyl probably affect the redox reaction time and then affect the cell reaction efficiency since the large numbers of eliminated protons is against the iodide ion attacking. This can explain the superiority of the N719 dye compared with the more carboxylic N3 dye from the view of the redox reactional activity and time. Iodide ion combined N3 molecule still has the ability to attract another iodide ion but the second iodide ion which attends the second redox reaction step will not approach the intermediums before the electronic excitation and injection. The iodide ion will also cause a red shift of N3 absorption spectra and it would probably contribute the absorption transition in lower energy region. This study clarify the behavior between neutral dye with deprotonation and redox couple before positively charged dye yield and our following work will investigate the regeneration of oxidized dye and excited dye comprehensively

■ ASSOCIATED CONTENT

Supporting Information

All the optimized geometries of N3−I serial and their interation energies. This material is available free of charge via the Internet at http://pubs.acs.org.

■ AUTHOR INFORMATION

Corresponding Authors

*E-mail: zhanghx@mail.jlu.edu.cn (H.-X.Z.). Telephone: +86-431-8849-8966 Fax: +86-431-8894-5942.
*E-mail: baifq@jlu.edu.cn (F.-Q.B.).

Notes

The authors declare no competing financial interest.

■ ACKNOWLEDGMENTS

This work was supported by the Natural Science Foundation of China (Grant No. 21003057 and 21173096) and Specialized Research Fund for the Doctoral Program of Higher Education (Grant 20110061110018) and the State Key Development Program for Basic Research of China (Grant 2013CB834801).

■ REFERENCES

(1) O'regan, B.; Grfitzeli, M. A Low-Cost, High-Efficiency Solar Cell Based on Dye-Sensitized. *Nature* **1991**, *353*, 24.
(2) Kalyanasundaram, K.; Grätzel, M. Applications of Functionalized Transition Metal Complexes in Photonic and Optoelectronic Devices. *Coord. Chem. Rev.* **1998**, *177* (1), 347−414.
(3) Hagfeldt, A.; Grätzel, M. Molecular Photovoltaics. *Acc. Chem. Res.* **2000**, *33* (5), 269−277.
(4) Grätzel, M. Photoelectrochemical Cells. *Nature* **2001**, *414* (6861), 338−344.
(5) Nazeeruddin, M. K.; Zakeeruddin, S.; Humphry-Baker, R.; Jirousek, M.; Liska, P.; Vlachopoulos, N.; Shklover, V.; Fischer, C.-H.; Grätzel, M. Acid-Base Equilibria of (2,2′-Bipyridyl-4,4′-Dicarboxylic Acid) Ruthenium (II) Complexes and the Effect of Protonation on Charge-Transfer Sensitization of Nanocrystalline Titania. *Inorg. Chem.* **1999**, *38* (26), 6298−6305.
(6) Nazeeruddin, M. K.; Kay, A.; Rodicio, I.; Humphry-Baker, R.; Müller, E.; Liska, P.; Vlachopoulos, N.; Grätzel, M. Conversion of Light to Electricity by Cis-X_2bis (2,2′-Bipyridyl-4, 4′-Dicarboxylate) Ruthenium (II) Charge-Transfer Sensitizers (X = Cl^-, Br^-, I^-, CN^-, and SCN^-) on Nanocrystalline Titanium Dioxide Electrodes. *J. Am. Chem. Soc.* **1993**, *115* (14), 6382−6390.
(7) Onozawa-Komatsuzaki, N.; Yanagida, M.; Funaki, T.; Kasuga, K.; Sayama, K.; Sugihara, H. Near-IR Dye-Sensitized Solar Cells Using A New Type of Ruthenium Complexes Having 2,6-Bis(quinolin-2-yl) Pyridine Derivatives. *Sol. Energ. Mat. Sol. C* **2011**, *95* (1), 310−314.
(8) Nazeeruddin, M. K.; Pechy, P.; Renouard, T.; Zakeeruddin, S. M.; Humphry-Baker, R.; Comte, P.; Liska, P.; Cevey, L.; Costa, E.; Shklover, V. Engineering of Efficient Panchromatic Sensitizers for Nanocrystalline TiO_2-Based Solar Cells. *J. Am. Chem. Soc.* **2001**, *123* (8), 1613−1624.
(9) Nazeeruddin, M. K.; De Angelis, F.; Fantacci, S.; Selloni, A.; Viscardi, G.; Liska, P.; Ito, S.; Takeru, B.; Grätzel, M. Combined Experimental and DFT-TDDFT Computational Study of Photoelectrochemical Cell Ruthenium Sensitizers. *J. Am. Chem. Soc.* **2005**, *127* (48), 16835−16847.
(10) Jang, S.-R.; Choi, M.-J.; Vittal, R.; Kim, K.-J. Anchorage of N3 Dye-Linked Polyacrylic Acid to TiO_2 Electrolyte Interface for Improvement in the Performance of a Dye-Sensitized Solar Cell. *Sol. Energ. Mat. Sol. C* **2007**, *91* (13), 1209−1214.
(11) Dai, F.-R.; Wu, W.-J.; Wang, Q.-W.; Tian, H.; Wong, W.-Y. Heteroleptic Ruthenium Complexes Containing Uncommon 5,5′-Disubstituted-2,2′-Bipyridine Chromophores for Dye-Sensitized Solar Cells. *Dalton Trans.* **2011**, *40* (10), 2314−2323.
(12) Wang, J.; Bai, F.-Q.; Xia, B.-H.; Feng, L.; Zhang, H.-X.; Pan, Q.-J. On the Viability of Cyclometalated Ru(II) Complexes As Dyes in DSSC Regulated by COOH Group, a DFT Study. *Phys. Chem. Chem. Phys.* **2011**, *13* (6), 2206−2213.
(13) Chen, J.; Bai, F.; Wang, J.; Sun, L.; Pan, Q.; Zhang, H. Theoretical Studies of the Structures and Spectroscopic Properties of The Photoelectrochemical Cell Ruthenium Sensitizers, C101 and J13. *Sci. Chin. Chem.* **2012**, *55* (3), 398−408.
(14) Li, M. X.; Zhou, X.; Xia, B. H.; Zhang, H. X.; Pan, Q. J.; Liu, T.; Fu, H. G.; Sun, C. C. Theoretical Studies on Structures and Spectroscopic Properties of Photoelectrochemical Cell Ruthenium Sensitizers, $Ru(H(M)Tcterpy)(NCS)_3^{N-}$ (M = 0, 1, 2, and 3; N = 4, 3, 2, and 1). *Inorg. Chem.* **2008**, *47* (7), 2312−2324.
(15) Rekhis, M.; Labat, F.; Ouamerali, O.; Ciofini, I.; Adamo, C. Theoretical Analysis of the Electronic Properties of N3 Derivatives. *J. Phys. Chem. A* **2007**, *111* (50), 13106−13111.
(16) Clifford, J. N.; Palomares, E.; Nazeeruddin, M. K.; Gratzel, M.; Durrant, J. R. Dye Dependent Regeneration Dynamics in Dye Sensitized Nanocrystalline Solar Cells: Evidence for the Formation of a Ruthenium Bipyridyl Cation/Iodide Intermediate. *J. Phys. Chem. C* **2007**, *111* (17), 6561−6567.
(17) Privalov, T.; Boschloo, G.; Hagfeldt, A.; Svensson, P. H.; Kloo, L. A Study of the Interactions between I^-/I_3^- Redox Mediators and Organometallic Sensitizing Dyes in Solar Cells. *J. Phys. Chem. C* **2009**, *113* (2), 783−790.
(18) Hu, C.-H.; Asaduzzaman, A. M.; Schreckenbach, G. Computational Studies of the Interaction between Ruthenium Dyes and X^- and X^{2-}, X = Br, I, At. Implications for Dye-Sensitized Solar Cells. *J. Phys. Chem. C* **2010**, *114* (35), 15165−15173.
(19) Lobello, M. G.; Fantacci, S.; De Angelis, F. Computational Spectroscopy Characterization of the Species Involved in Dye Oxidation and Regeneration Processes in Dye-Sensitized Solar Cells. *J. Phys. Chem. C* **2011**, *115* (38), 18863−18872.
(20) Kusama, H.; Sayama, K. Effect of Side Groups for Ruthenium Bipyridyl Dye on the Interactions with Iodine in Dye-Sensitized Solar Cells. *J. Phys. Chem. C* **2012**, *116* (1), 1493−1502.
(21) Kusama, H.; Sugihara, H.; Sayama, K. Theoretical Study on the Interactions between Black Dye and Iodide in Dye-Sensitized Solar Cells. *J. Phys. Chem. C* **2011**, *115* (18), 9267−9275.
(22) Chen, J.; Bai, F.-Q.; Wang, J.; Hao, L.; Xie, Z.-F.; Pan, Q.-J.; Zhang, H.-X. Theoretical Studies on Spectroscopic Properties of Ruthenium Sensitizers Absorbed to TiO_2 Film Surface with Connection Mode for DSSC. *Dyes Pigm.* **2012**, *94* (3), 459−468.
(23) Zhao, Y.; Truhlar, D. G. The M06 Suite of Density Functionals for Main Group Thermochemistry, Thermochemical Kinetics, Noncovalent Interactions, Excited States, and Transition Elements: Two New Functionals and Systematic Testing of Four M06-Class

Functionals and 12 Other Functionals. *Theor. Chem. Acc.* **2008**, *120* (1−3), 215−241.
(24) Yanai, T.; Tew, D. P.; Handy, N. C. A New Hybrid Exchange−Correlation Functional Using the Coulomb-Attenuating Method (CAM-B3LYP). *Chem. Phys. Lett.* **2004**, *393* (1), 51−57.
(25) Xu, X.; Zhang, Q.; Muller, R. P.; Goddard, W. A., III An Extended Hybrid Density Functional (X3LYP) with Improved Descriptions of Nonbond Interactions and Thermodynamic Properties of Molecular Systems. *J. Chem. Phy.* **2005**, *122*, 014105.
(26) Josa, D.; Rodríguez-Otero, J.; Cabaleiro-Lago, E. M.; Rellán-Piñeiro, M. Analysis of the Performance of DFT-D, M05-2X and M06-2X Functionals for Studying II···II Interactions. *Chem. Phys. Lett.* **2013**, *557* (0), 170−175.
(27) Hohenstein, E. G.; Chill, S. T.; Sherrill, C. D. Assessment of the Performance of the M05-2X and M06-2X Exchange-Correlation Functionals for Noncovalent Interactions in Biomolecules. *J. Chem. Theory. Comput.* **2008**, *4* (12), 1996−2000.
(28) Gu, J.; Wang, J.; Leszczynski, J. Stacking and H-Bonding Patterns of Dgpdc and Dgpdcpdg: Performance of the M05-2X and M06-2X Minnesota Density Functionals for the Single Strand DNA. *Chem. Phys. Lett.* **2011**, *512* (1−3), 108−112.
(29) Reed, A. E.; Curtiss, L. A.; Weinhold, F. Intermolecular Interactions from a Natural Bond Orbital, Donor-Acceptor Viewpoint. *Chem. Rev.* **1988**, *88* (6), 899−926.
(30) Frisch, M.; Trucks, G.; Schlegel, H. B.; Scuseria, G.; Robb, M.; Cheeseman, J.; Scalmani, G.; Barone, V.; Mennucci, B.; Petersson, G.; Gaussian 09, Revision A. 1. Gaussian Inc.: Wallingford, CT, 2009.
(31) Bondi, A. Van Der Waals Volumes and Radii. *J. Phys. Chem.* **1964**, *68* (3), 441−451.